Editor: Dr Renu Bharadwaj

Journal Pre-proof

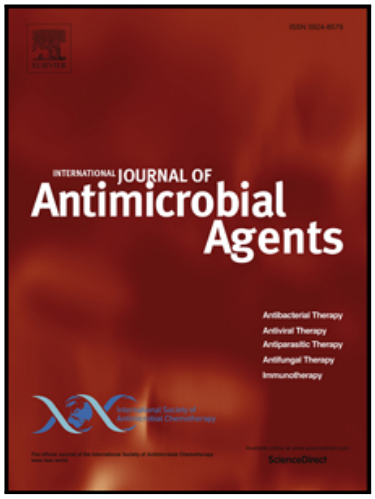

The novel drug candidate VOMG kills Mycobacterium abscessus and other pathogens by inhibiting cell division

Giulia Degiacomi , Laurent R. Chiarelli , Olga Riabova , Nicola Ivan Loré , Lara Muñoz-Muñoz , Deborah Recchia , Giovanni Stelitano , Umberto Postiglione , Fabio Saliu , Anna Griego , Viola Camilla Scoffone , Elena Kazakova , Edoardo Scarpa , José Manuel Ezquerra-Aznárez , Alessandro Stamilla , Silvia Buroni , Enrico Tortoli , Loris Rizzello , Davide Sassera , Santiago Ramon-Garcia , Daniela Maria Cirillo , Vadim Makarov , Maria Rosalia Pasca

PII: S0924-8579(24)00196-1
DOI: https://doi.org/10.1016/j.ijantimicag.2024.107278
Reference: ANTAGE 107278

To appear in: *International Journal of Antimicrobial Agents*

Received date: 5 April 2024
Accepted date: 16 July 2024

Please cite this article as: Giulia Degiacomi , Laurent R. Chiarelli , Olga Riabova , Nicola Ivan Loré , Lara Muñoz-Muñoz , Deborah Recchia , Giovanni Stelitano , Umberto Postiglione , Fabio Saliu , Anna Griego , Viola Camilla Scoffone , Elena Kazakova , Edoardo Scarpa , José Manuel Ezquerra-Aznárez , Alessandro Stamilla , Silvia Buroni , Enrico Tortoli , Loris Rizzello , Davide Sassera , Santiago Ramon-Garcia , Daniela Maria Cirillo , Vadim Makarov , Maria Rosalia Pasca , The novel drug candidate VOMG kills Mycobacterium abscessus and other pathogens by inhibiting cell division, *International Journal of Antimicrobial Agents* (2024), doi: https://doi.org/10.1016/j.ijantimicag.2024.107278

Highlights

- VOMG is a drug-like molecule discovered against *Mycobacterium abscessus*.
- VOMG has also a broad-spectrum activity against other microbial pathogens.
- It has a new mode of action inhibiting cell division, in particular FtsZ activity.
- VOMG is active against *M. abscessus in vitro, in vivo* and against biofilm.
- It is a water-soluble anti-*M. abscessus* compound with good ADME/Tox properties.

The novel drug candidate VOMG kills *Mycobacterium abscessus* and other pathogens by inhibiting cell division

Giulia Degiacomi[a, †], Laurent R. Chiarelli[a,†], Olga Riabova[b,†], Nicola Ivan Loré[c,†], Lara Muñoz-Muñoz[d,†], Deborah Recchia[a], Giovanni Stelitano[a], Umberto Postiglione[a], Fabio Saliu[c], Anna Griego[e,f], Viola Camilla Scoffone[a], Elena Kazakova[b], Edoardo Scarpa[e,f], José Manuel Ezquerra-Aznárez[d], Alessandro Stamilla[a], Silvia Buroni[a], Enrico Tortoli[c], Loris Rizzello[e,f], Davide Sassera[a,g], Santiago Ramon-Garcia[d,h,i,*], Daniela Maria Cirillo[c,*], Vadim Makarov[b,*], Maria Rosalia Pasca[a,g,*]

[a] Department of Biology and Biotechnology "Lazzaro Spallanzani", University of Pavia; via Ferrata 9, 27100 Pavia, Italy

[b] Federal Research Centre "Fundamentals of Biotechnology" of the Russian Academy of Sciences (Research Centre of Biotechnology RAS); 33-2 Leninsky Prospect, 119071 Moscow, Russia

[c] Emerging Bacterial Pathogens Unit, Division of Immunology, Transplantation and Infectious Disease, IRCCS San Raffaele Scientific Institute; via Olgettina 60, 20132 Milano, Italy

[d] Dep. Microbiology/Fac. Medicine, University of Zaragoza; C/ Pedro Cerbuna 12, 50009 Zaragoza, Spain

[e] Department of Pharmaceutical Sciences, University of Milan; Via Mangiagalli 25, 20133 Milano, Italy

[f] The National Institute of Molecular Genetics (INGM); via Francesco Sforza, 35, 20122 Milano, Italy

[g] Fondazione IRCCS Policlinico San Matteo; Viale Camillo Golgi 19, 27100 Pavia, Italy

[h] Research and Development Agency of Aragon Foundation (ARAID Foundation); Av. de Ranillas 1-D, 50018 Zaragoza, Spain

[i] Spanish Network for Research on Respiratory Diseases (CIBERES), Carlos III Health Institute; 28029 Madrid, Spain

[†] These authors contributed equally to this work.

[*] **Corresponding authors**: mariarosalia.pasca@unipv.it (M.R. Pasca); makarov@inbi.ras.ru (V. Makarov); cirillo.daniela@hsr.it (D. Cirillo); santiramon@unizar.es (S. Ramon-Garcia).

Running title: The first new drug-like anti-*Mycobacterium abscessus* compound targeting cell division.

Abstract counts: 181/200

Number of figures: 5

Number of supplementary Figures: 4

Number of supplementary Tables: 13

ABSTRACT

Aims: The incidence of lung infections is increasing worldwide in individuals suffering from cystic fibrosis and chronic obstructive pulmonary diseases. *Mycobacterium abscessus* is associated to chronic lung deterioration in these populations. The intrinsic resistance of *M. abscessus* to most conventional antibiotics jeopardizes treatment success rates. To date no single drug has been developed targeting specifically *M. abscessus.* Our objective was to characterize the pyrithione-core drug-like small molecule named VOMG as a new compound active against *M. abscessus* and other pathogens.

Methods: We used a multidisciplinary approach including microbiological, chemical, biochemical and transcriptomics procedures to validate VOMG as a promising anti-*M. abscessus* drug candidate.

Results: We report for the first time the *in vitro* and *in vivo* bactericidal activity of VOMG against *M. abscessus* and other pathogens. Besides being active against *M. abscessus* biofilm, the compound showed a favourable pharmacology (ADME-Tox) profile. Frequency of resistance studies were unable to isolate resistant mutants. VOMG inhibits cell division, particularly the FtsZ enzyme.

Conclusions: VOMG is a new drug-like molecule discovered against *M. abscessus* inhibiting cell division with broad spectrum activity against other microbial pathogens.

Keywords: *Mycobacterium abscessus*, cell division, FtsZ, nontuberculous mycobacterium

1. Introduction

Mycobacterium abscessus subsp. *abscessus* (*Mab*, also known as *Mycobacteroides abscessus* subsp. *abscessus*) is an opportunistic pathogen that has recently emerged as responsible for a wide range of clinical manifestations [1-3]. The incidence of *Mab* caused pulmonary infections is on the rise worldwide and deserves special attention in people with cystic fibrosis (CF) and chronic obstructive pulmonary disease (COPD) [4,5].

Mab is intrinsically resistant to many drugs mainly due to the presence of the mycobacterial cell wall with low permeability. It is primarily composed of lipids, like mycolic acids (up to 60%) [6]. Furthermore, unlike *Mycobacterium tuberculosis*, *Mab* is characterized by two morphotypes: smooth (S) and rough (R) [6]. In *Mab* pulmonary infection, S strains producing glycopeptidolipids first colonize the lung epithelium and form biofilm [3,7,8]. It is noteworthy that *Mab* biofilms are particularly tolerant to antibiotics, contributing to their drug resistance [3,6,9]. From S strains, rough cord-forming variants could emerge, which are more virulent, and which cause invasive lung infections [3,6,7].

Current anti-*Mab* therapies rely on old drugs and have very poor success rates [10,11]. One of the reasons is that *Mab* is highly resistant to the currently used antimicrobial drugs [12] and no new antibiotics have been specifically developed for this pathogen [13,14]. Treatment failure leads to an accelerated decline in lung function and, in some countries, *Mab*-infected CF individuals are excluded from lung transplantation lists [3-5]. Recently, kaftrio (Elexacaftor/tezacaftor/ivacaftor) was introduced as CFTR gene therapy for selected people with CF. Some studies reported that kaftrio treatment can reduce *Mab* infection because either it improves the pathology (less mucus on the lung) or it restores the innate immune function against the pathogen [15,16].

There is therefore a crucial need to develop new *Mab*-specific drugs with a novel mechanism of action to be effective against these multidrug-resistant strains.

The anti-*Mab* drug pipeline is narrowly focused on repurposing or reformulating approved antibiotics for other indications (e.g.: bedaquiline, rifabutin, etc. used in tuberculosis (TB) therapy), reminiscent of the dry pipeline scenario in TB research two decades ago [13,14]. However, a few repurposed drugs active against *Mab* have been identified in the last few years such as the antimalarial OZ439 (targeting DosS-mediated hypoxic signalling), third-generation tetracyclines, the new β-lactam T405 and an epetraborole analog inhibiting the leucyl-tRNA synthetase [17-20]. Furthermore, some new antitubercular compounds have been shown to be also active against *Mab* [21,22]. Recently, activity against *Mab* was shown for the non drug like polycationic compound COE-PNH2 [23].

Mab infections are often complicated by co-infections with other pathogens, especially in CF individuals. A drug inhibiting novel bacterial targets embedded in conserved pathways/functions could therefore be beneficial in such situations.

In recent years, bacterial cell division (CD) has emerged as a critical target in drug discovery [24]. Conserved proteins involved in CD, which often have no counterpart in eukaryotic cells (or low homology), are essential for bacterial survival and have been extensively studied [24,25]. FtsZ is highly conserved due to its essential role in CD [26] and it is considered an interesting cellular target for drugs with a broad spectrum of action. FtsZ protein is a structural homolog of the eukaryotic tubulin; both proteins are polymerised in a GTP-dependent manner to form cytoskeletal filaments for CD, but they have different functions [26,27].

FtsZ has been extensively investigated as a potential target of antimycobacterial compounds, and several molecules specifically targeting the *M. tuberculosis* enzyme have been reported to act

through different mechanisms of action, such as by interference with polymerization or assembly of FtsZ or inhibiting GTPase activity [28]. Moreover, some FtsZ inhibitors have been identified with anti-*Mab in vitro* activity [29,30] but have not been further characterized. Thus, despite the high "druggability" of this enzyme, currently, there are no FtsZ inhibitors in the *Mab* drug development pipeline [13].

In this work, we identified a new pyrithione-core molecule, named VOMG, primarily active against *Mab*, but also against other relevant pathogens including *Mycobacterium tuberculosis* (*Mtb*) and *Staphylococcus aureus* (*Sau*). Employing a multidisciplinary approach, we showed that VOMG displays a potent *in vitro* bactericidal activity against *Mab* in both planktonic and biofilm growth, and in an *in vivo* mouse model of *Mab* infection. Furthermore, using transcriptomic, biochemical and microbiological approaches we showed that VOMG inhibits CD, in particular FtsZ activity.

2. Methods

2.1. High-resolution confocal microscopy for single-cell analysis

Mab ATCC 19977 cells were grown in Middlebrook 7H9 broth at 37°C in shaking condition (150 rpm) to mid-log phase (OD_{600} 0.5-0.8) before snapshot single-cell assay. Fluorescence snapshot imaging was acquired using a 63x glycerol immersion objective installed on an inverted STELLARIS 8 Confocal Microscopy equipped with a 410 to 850 tunable pulsed white laser. Samples for imaging were prepared dispensing 0.5 μL of batch culture between two #1.5 coverslips. Exponential-phase *Mab* cells were either treated or not with 50 μg/mL of VOMG for 4

and 24 hours. To accurately monitor the bacterial changes induced by VOMG treatment, we employed two chemical dyes staining *Mab* chromosome (Hoechst), to observe possible DNA condensation or the presence of multiple bacterial chromosomes within the same cells, and the FM™ 1-43 to label mycobacterial membrane. At each mentioned time point, 1 mL of culture was used to perform a staining of the bacterial chromosome using Hoescht (1:1000) and the mycobacterial membrane using the FM™ 1-43 dye (1:1000) (ThermoFisher) for 15 minutes at room temperature. Then, the stained samples were washed once and resuspended in 50 µL of PBS. ROI Manager Macro of ImageJ2 (Fiji) 2.9.0/1.53t software [31] was used to perform single-cell segmentation. The selection brush tool was used to cover the profile of individual cells and extract bacterial length and area.

2.2. Biochemical assays with FtsZ proteins

For both *Mab* and *Sau* enzymes, the GTPase activity was performed at 30°C, with spectrophotometric coupled assay using pyruvate kinase and L-lactate dehydrogenase (PK/LDH) as previously described [32]. For GTPase inhibition assays, the enzymatic activity was determined in the presence of increasing concentrations of VOMG (0.5-100 µM) and the IC_{50} was determined using equation (1) and GraphPad Prism 9:

$$\text{Eq. 1} \qquad A_{[I]} = A_{[0]} \times \left(1 - \frac{[I]}{[I]+IC_{50}}\right).$$

$A_{[I]}$: activity of the enzyme at inhibitor concentration [I]; $A_{[0]}$: activity of the enzyme without inhibitor.

The FtsZ inhibitor C109 [29, 33] was used as a positive control (Data not shown).

The *Sau* FtsZ polymerization assay was performed by sedimentation assay, as previously described [33]. Briefly, the assay was done in 50 mM MES pH 6.5, 5 mM $Mg(CH_3COO)_2$, 100 mM

CH_3CO_2K, with 12 μM FtsZ, and 2 mM GTP or GDP. The reaction was incubated at 30°C and 300 rpm for 10 min, then samples were centrifuged (350000× *g*, 10 min, 25°C). The supernatant was immediately separated from the pellet containing the protein polymers, and the samples were analysed by 12% SDS-PAGE, with Blue Coomassie staining. The *Mab* FtsZ sedimentation assay was performed as above, but in 50 mM MES pH 6.5, 5 mM $MgCl_2$, 50 mM KCl. In both cases, the polymerization assays were conducted in the presence of different VOMG concentrations (1-100 μM).

Light scattering assay of FtsZ polymerization was performed as previously described, by measuring the 90° angle light scattering with a Cary Eclipse Fluorescence Spectrophotometer (Varian), and using both excitation and emission wavelengths at 400 nm [32]. The polymerization was measured at 30°C, in 150 μL of 50 mM MES pH 6.6, 10 mM $Mg(CH_3COO)_2$, 100 mM CH_3CO_2K, using FtsZ at a final concentration of 12.5 μM, after addition of 1 mM GTP, and data was collected every 5 s.

2.3. In vivo efficacy studies of VOMG in mice

Mice were housed (3-5 mice per cage) in the biosafety level 3 (BSL-3) animal facility at IRCCS San Raffaele Scientific Institute (Milano, Italia). Lung infection was established to test the *in vivo* VOMG efficacy using an agar beads C57BL/6 mouse *Mab* infection model [34-36]. Briefly, *Mab* colonies from 7H10 plates were grown for 2 days (to reach exponential phase) in 20 mL of Middlebrook 7H9 broth. For bead preparation, 50 mL of white heavy mineral oil and 25 mL of Trypticase soy agar (TSA) were added to a bacterial suspension, reaching an OD_{600} of 15, and mixed at medium speed with a magnet on a stirrer to generate agar beads, as previously described [37]. Agar bead preparations were stored at 4°C for no more than a week; fresh preparations were

performed every time. The incorporation of *Mab* in agar beads and the intratracheal injection allowed to physically retain the bacteria in the bronchial airways providing microanaerobic/anaerobic conditions which allow bacteria to grow in microcolonies [34-36]. For the infection, mice were anaesthetized, and the trachea was exposed and intubated, then the bead suspension (50 μL, 1×10^5 CFU) was injected and the incision closed with suture clips. Mice intratracheally infected with *Mab* ATCC19977 ($1x10^5$ CFU) were treated daily with vehicle (saline solution), amikacin (intraperitoneal administration, IP: 100 mg/kg mice, as positive control group) and VOMG by intranasal administration for seven consecutive days, as previously described [36]. At the end of treatment (8 days post challenge), mice were euthanized, and lungs were excised aseptically and homogenized in 2 mL PBS using the homogenizer gentleMACSTM Octo Dissociator. Bacterial loads in local (lung homogenates) and systemic compartments (blood) were determined by plating the samples at 10-fold serial dilution in 7H10 agar medium (BD Difco). The experiment was repeated three times.

2.4. Statistical analysis

For biofilm confocal analysis, images were processed with Image J software and statistical analysis was carried out with Prism 8 (GraphPad Software) using Mann-Withney test. P values < 0.05 were considered significant.

For single cell analysis, plots and statistical analysis were generated using Prism 9.4 (GraphPad Software). Welch t-test was performed to compare the variation of a single parameter over multiple groups. P values < 0.05 were considered significant.

Mann-Whitney tests were performed to compare the variation of a single parameter over multiple groups in *in vivo* experiments. P values < 0.05 were considered significant.

3. Results

3.1. Discovery of VOMG as a potent inhibitor of Mab growth

Based on the idea that compounds active against *Mab* may sometimes originate from anti-tuberculosis drug discovery campaigns, we synthesized a range of small-molecule derivatives from the class of pyridine 1-oxides, previously recognized for its *in vitro* activity against *Mtb* [38]. We showed that all these new derivatives exhibited moderate activity against *Mab* ATCC 19977 growth with a minimal inhibitory concentration (MIC) ranging from 1 to 2 µg/mL. Structurally, they shared two common structural features: electron-withdrawing groups at position 5 and a carbamimidoylthio fragment (Supplementary Table S1). We hypothesized that these compounds may act as prodrugs and could be transformed into the same active metabolite that is responsible for their *in vitro* activity against *Mab*. To confirm this hypothesis, we further studied x-VOMG, which is one of the active derivatives, and its two putative degradation products, VOMG and RCB19348 (Supplementary Table S1; Fig. 1 A).

Non-pathogenic *Mycobacterium smegmatis* cultures were incubated in the presence of x-VOMG (MIC = 2.5 µg/mL) and analysed by thin-layer chromatography (TLC); x-VOMG was almost completely degraded in the *M. smegmatis* cell extract, and a spot migrating as VOMG base occurred (Fig. 1 B, C). Similar results were obtained when both compounds were incubated in 7H9 medium only, suggesting spontaneous hydrolysis of x-VOMG to VOMG base in aqueous media, as confirmed by mass spectrometry analysis (Fig. 1 D-F). These data showed that x-VOMG, and probably all our pyrithione-based derivatives, are prodrugs converted to the same 5-(ethoxycarbonyl)-2-sulfidopyridine 1-oxide, named VOMG base (the corresponding sodium salt was called VOMG).

VOMG demonstrated higher activity against *Mab* (MIC = 0.125-0.250 µg/mL) whereas RCB19348 was inactive (Fig. 1 A; Supplementary Table S1). Structure-activity relationship studies of VOMG revealed that the sulphide substituent is preferable for the anti-*Mab* activity rather than the thiocyanate or sulfone substituents. RCB12083 and RCB13031 showed equipotent activity as VOMG, while RCB99063 and RCB12146 displayed diminished activity, and RCB12155 was completely inactive (Supplementary Table S1). Consequently, VOMG was chosen for further studies due to its water-soluble properties, as described in "Chemistry section" of Supplementary materials.

3.2. VOMG has bactericidal and anti-biofilm activity against Mab, and is suitable for drug combination therapy

Time-kill assays (TKA) using the reference *Mab* ATCC 19977 strain demonstrated a rapid bactericidal activity of VOMG against *Mab* planktonic cells with an early onset of activity (after 24 hours) and sterilizing capacity (no regrowth after 14 days of incubation) with a clear concentration cut-off at 1X MIC values (0.250 µg/mL) (Fig. 2 A). This represents an improvement compared to most drugs used in *Mab* therapy that are bacteriostatic [3,13]; amikacin, tigecycline, levofloxacin, imipenem, clofazimine and linezolid also showed a bactericidal effect at the highest concentrations (typically 4X MIC and 10X MIC) but with slow onset of activity or no sterilizing capacity (Fig. 2 A; Supplementary Fig. S1).

The antibiofilm activity of VOMG was determined following previously described protocols [39] using a high initial inoculum of 10^8 cells/mL to facilitate biofilm formation. Biofilm studies showed a VOMG minimal bactericidal eradication concentration (MBEC) of 128 µg/mL, similar to clarithromycin and amikacin used as positive controls (Fig. 2 B). Further studies by confocal

laser scanning microscopy (CLSM) showed that biofilm formation was significantly prevented by VOMG (8 µg/mL), similar to clarithromycin, measured as reduction in the biofilm thickness and covered surface (Fig. 2 C). When a mature biofilm was treated with VOMG (80 µg/mL) the thickness of the mature biofilm was reduced although the covered surface remained constant. Clarithromycin decreased the covered surface of the mature biofilm but had no effect on the biofilm thickness, while amikacin had no activity against *Mab* biofilms. The three compounds had a reduced effect against a mature biofilm at lower concentration (8 µg/mL) (Supplementary Fig. S2).

The potential inclusion of VOMG in combinational *Mab* therapy was evaluated by combinatorial TKA assay with nine currently used anti-*Mab* compounds. No antagonism was identified, indicating the suitability of VOMG for combination therapy (Supplementary Fig. S3).

3.3. VOMG displays broad-spectrum antibacterial activity and is active against drug-resistant clinical isolates

The water soluble VOMG molecule (Supplementary Table S1) showed greater activity than its prodrug x-VOMG against all the mycobacterial species tested, including *Mab*, *Mycobacterium avium* and *Mtb* drug resistant isolates (Supplementary Table S2). VOMG was also active against *Escherichia coli*, *Acinetobacter baumannii* and *Sau*, including methicillin-resistant clinical isolates (Supplementary Table S3), while it was inactive against *Klebsiella pneumoniae* and *Pseudomonas aeruginosa* (MIC > 128 µg/mL). However, activity against *P. aeruginosa* could be restored in the presence of the efflux pump inhibitor PaßN (MIC = 1 µg/mL). VOMG was also active against some fungal species (Supplementary Table S4).

3.4. VOMG has favourable ADME-Tox profile and shows efficacy in a mouse model of Mab infection

VOMG revealed good metabolic stability in mouse and human liver microsomes, low levels of CYP inhibition, no mutagenicity (Ames fluctuation test) and no cardiotoxicity (hERG assay) signals (Supplementary Table S5).

A chronic toxicity study in healthy C57BL/6 male mice following a single oral administration of VOMG (50 mg/kg) showed no adverse effects during the two-week observation period (Supplementary Table S6). The acute toxicity study in mice showed an LD_{50} dose of 455.78±21.79 mg/kg.

Pharmacokinetics studies in mice revealed a good bioavailability of VOMG. Peak plasma concentrations were achieved after 4 hours following a single oral administration. VOMG was gradually eliminated with a mean retention time of 18.3 hours and a half-life of 12.3 hours. The apparent volume of distribution was established as 273.6 mL/g and apparent total body clearance was 15.38 mL/h/g (Fig. 3 A; Supplementary Table S7).

The *in vivo* efficacy of VOMG was tested using different doses (50, 100 and 500 mg/kg bw) in C57BL/6NCrl mice infected with agar-embedded *Mab* cells. Intranasal administration of VOMG at the lowest dose tested (50 mg/kg bw) significantly reduced the bacterial load in the lungs and at systemic levels in blood samples in comparison to the control untreated infected groups. The results were comparable to those observed in the positive control group treated with amikacin (Fig. 3 B-D).

3.5. VOMG and its prodrug inhibit cell division

To study VOMG mechanism of action, first we tried to generate *in vitro* VOMG resistant mutants in *Mab*, *Mtb* and in *M. smegmatis* using a strain lacking NucS/EndoMS [40]. All attempts were unsuccessful, suggesting a cellular target essential for mycobacterial cell growth. Then, we screened a panel of *Mtb* mutants resistant to known drugs, which harbour identified mutations in genes encoding targets [41-44] activators [43,45] and associated mechanisms of drug resistance [43,46,47]; these strains were all sensitive to VOMG (Supplementary Table S8), suggesting a different mechanism of resistance as the ones represented in the panel.

Finally, *Mab* cultures treated with x-VOMG (10- and 20-fold MIC, plus untreated controls) were subjected to transcriptomics to identify differentially expressed genes (DGEs). In total, 493 genes were found to be differentially expressed in both treatments compared to controls: 363 up-regulated and 130 down-regulated (Supplementary Table S9) (Fig. 4 A-C). The level of expression of three DGEs (two induced and one repressed) was also confirmed by quantitative real-time PCR (Supplementary Table S10). Assignment of *Mab* ATCC 19977 genes to functional categories revealed that most DGEs fall within seven functional categories [48]: the most represented groups were “conserved hypothetical proteins” and “intermediary metabolism and respiration” (Fig. 4 C). The most overexpressed genes were associated with compound-induced stress, such as genes encoding catalase, carbonic anhydrase (*MAB_3211c*), kinase, and alternative sigma factors [49]. Interestingly, we found overexpression of several genes encoding proteins involved in metal metabolism (e.g.: ArsR, ArsC, etc.), nitrogen and sulphur metabolism and membrane proteins (e.g.: efflux pumps, chaperonines and heat shock proteins) (Fig. 4 C). These data suggested that x-VOMG treatment could cause cellular stress, affecting cell permeability and disrupting metal homeostasis.

Genes involved in transcription, protein and ATP synthesis processes were shut-down by x-VOMG treatment (genes encoding RNA polymerase subunits like *rpoB*; RHO factor and NusG factor; ribosomal proteins like *rpmI*, *rpmT*, *rpmD*; translation initiation factors; the operon coding for ATP synthase) [50,51]. Cellular respiration was also inhibited (e.g.: genes encoding quinones and cytochromes), as well as genes encoding MCE proteins, promoting macrophage invasion [52]. Interestingly, the most downregulated operon was the highly conserved division cell wall (*dcw*) operon essential for *Mab* growth. Genes coding for FtsZ, FtsQ, SepF (positive CD regulator), SteA and SteB (involved in the last CD steps), MurC and MurG (involved in peptidoglycan biosynthesis) were downregulated (Supplementary Table S11).

Our findings suggest that x-VOMG, and consequently its active metabolite VOMG, could inhibit CD, particularly FtsZ.

We thus monitored the morphological *Mab* single-cell changes (i.e., area and length) induced by VOMG (50 µg/mL, 200X MIC) after 4 and 24 hours of treatment (Fig. 4 D, E). Single cells analysis revealed that in particular after 24 hours of VOMG treatment, *Mab* cells exhibited a significant increase in both bacterial area and length compared to the untreated control (Fig. 4 D, E). In addition, the bacterial septum (white arrow in Fig. 4 D) could be observed in the 4-hours VOMG treated cells together with multiple condensation foci, conformation putatively compatible with the presence of multiple copies of the chromosome [53], suggesting an interruption in mycobacterial replication (Fig. 4 D). Similarly, an aberrant elongation, increased area and multiple chromosome foci within the same cell were observed in the 24-hour-treated cells (Fig. 4 E). These results confirm our RNA-seq findings indicating that VOMG dysregulates *Mab* CD.

3.6. VOMG inhibits FtsZ activity not only in Mab, but also in Sau through different mechanisms

We recombinantly produced *Mab* and *Sau* [33] FtsZ (Fig. S4) and evaluated the ability of VOMG to directly inhibit FtsZ GTPase activity and its ability to form polymers. VOMG was able to block FtsZ GTPase activity, although displaying only weak effects (IC_{50} values of 54.0 ± 3.6 μM and 18.5 ± 1.8 μM for *Mab* and *Sau* FtsZ, respectively) (Fig. 5 A, B). Thus, we tested whether VOMG could interfere directly with FtsZ polymerization. An *in vitro* sedimentation assay demonstrated that VOMG inhibited the formation of *Mab* FtsZ polymers in a concentration-dependent manner (Fig. 5 C). This was in contrast with the effect observed against the *Sau* FtsZ where the quantity of the polymerized protein increased (Fig. 5 D), suggesting that the effect of VOMG on FtsZ polymerization differs in the two pathogens. So, while in *Mab* polymer formation is inhibited, in *Sau* VOMG modified polymerization kinetics, increasing the quantity of polymers formed or affecting the polymers stability.

This evidence was confirmed by FtsZ polymerization kinetic studies through 90° light scattering assays. In *Mab*, VOMG initially induced very rapid FtsZ polymerisation, probably leading to unstable polymers that collapsed rapidly; the protein was no longer able to form polymers at the highest concentrations (Fig. 5 E). By contrast, in *Sau* FtsZ polymerized faster, but the depolymerization rate decreased, consequently the polymer disassembly was longer than the untreated control (Fig. 5 F). Our data thus confirmed that in both species the FtsZ polymer assembly and, consequently, the bacterial CD were dramatically impacted by VOMG.

4. Discussion

Over the last 15 years, *Mab* has emerged as a worrying pathogen causing several clinical manifestations and in particular lung infections in individuals suffering from CF and COPD. In these populations, *Mab* infection treatment outcomes are usually poor [3-5]. Unfortunately, the

elevated rates of attrition in the drug development process are directly linked to the limited options available in the anti-*Mab* drug pipeline. In fact, currently recommended and available therapeutic strategies are mainly based on repositioning antibiotics used for other indications, such as TB, and there are no specific new drugs on the horizon that can prevent *Mab* from becoming the next superbug [13,14]. Innovative approaches such as phage therapy can represent alternative therapies, although its wide clinical implementation remains a challenge, leaving options for personalized medicine [54].

VOMG was discovered in a focused screening to identify novel compounds active against *Mab* (1 compound active against *Mab* growth/ more than 700 tested; MR Pasca, V. Makarov, personal communication). VOMG is a highly polar molecule that has positive and negative centres as well as hydrophilic and lipophilic moieties in its structure. For these reasons, it can easily cross mycobacterial cell wall, like isoniazid. Furthermore, like drugs targeting enzymes located inside the cell, VOMG has hydrophilic moieties. Lipophilicity may be a key factor for antitubercular agents that target enzymes in the cell membrane [55,56]. Then, VOMG fully complies with Lipinski's rules: it has less than 5 donor hydrogen bonds; less than 10 acceptor hydrogen bonds; molecular weight less than 500; and octanol-water distribution coefficient less than 5.

VOMG is a pyrithione-core small molecule (x-VOMG is its prodrug) with a strong substituent at position 5 of the ring that withdraws electrons from sulfur and makes any chelation of metals other than copper unattainable (according to the Irving-Williams series of metal complex stability). Many drugs in the market can chelate copper and, very often, it corresponds to their toxicity-related mechanism of action towards bacterial cells [57,58]. In the case of VOMG, its preliminary safety profile was demonstrated through various assays, including *in vitro* and *in vivo* studies such as ADME-Tox assays and acute and subchronic toxicity studies in mice. In fact, pharmacokinetic and

toxicity studies using an oral dose of 100 mg/kg bw showed no toxicity and high safety (mean Cmax value of 400 ng/mL, above the MIC value of 250 ng/mL). ADME studies confirm the lack of toxicity signals in VOMG. In our *in vivo* studies, intranasal delivery directly into the lungs might have further increased concentration values directly in the site of infection, reducing systemic toxicity. Finally, VOMG could be suitable for novel drug delivery formulations, including aerosol inhalation [59], owing to its favourable physicochemical properties, such as water solubility, good oral bioavailability, and absence of toxicity [60].

The average success rate of *Mab* drug therapy is about 45% [61], as most drugs used as anti-*Mab* therapeutics are bacteriostatic [3,62], they have no anti-biofilm activity and are ineffective against drug-resistant isolates of this pathogen. In contrast, VOMG exhibits high bactericidal activity *in vitro*, eradicating *Mab* in planktonic culture, and anti-biofilm properties. It is also active against drug-resistant *Mab* clinical isolates, including multidrug-resistant (MDR) strains. Time-kill assays showed a clear concentration cut-off with lack of dose range correlation with activity. At a concentration of just 1X MIC values (0.25 µg/mL), VOMG rapidly reduced the bacterial load and cleared the culture. This activity was more potent than that of the currently recommended clarithromycin and amikacin or of other drugs under development [63]. VOMG was also equally or more active than the standard of care drugs against *Mab* in biofilm. Indeed, only a few compounds are active against *Mab* biofilm, such as clarithromycin, which was used in this study as control [64]. The anti-biofilm activity was observed using two complimentary approaches: prevention of biofilm formation and treatment of a mature biofilm. VOMG is also active against drug-resistant *Mab* clinical isolates, including MDR strains. Furthermore, we were unable to isolate mutants resistant to VOMG *in vitro*, which is a key aspect for infectious drug development, and is one of the most advantageous VOMG features.

The bactericidal and eradicating properties of VOMG, together with its broad-spectrum antimicrobial activity and anti-biofilm properties strongly reinforce the potential of VOMG in the treatment of pulmonary infections especially in CF individuals, even when the standard of care treatment is not effective.

A significant roadblock in the development of novel drugs against *Mab* is the absence of a validated mouse model of chronic *Mab* pulmonary disease suitable for evaluating the *in vivo* efficacy of novel therapeutics. BALB/c mice high dose intranasally infected produced an infection that progressed to ~ 10^7 CFU/ml in the lungs after 14 days post-infection [63]. C3HeB/FeJ mice aerosol-infected and treated with corticosteroids consent progression of the infection, reaching moderate bacterial burdens (~ 4-5 log10 CFU/mL in the lungs), but allowing for extended 4-weeks treatment schedules [65,66]. In our study, we used an alternative C57BL/6 model of *Mab* infection embedded within agar beads and directly delivered to the bronchial airways providing microanaerobic/anaerobic conditions that allow bacteria to grow in microcolonies [34-36], more accurately resembling the natural lung environment in CF individuals. In this model, a seven-day intranasal treatment of VOMG was able to contain the bacterial burden in the lungs and systemic (blood) similar to the effect achieved with amikacin (used as control), which was administered intraperitoneally. The VOMG water solubility, coupled with the *in vivo* findings by the intranasal administration could allow to speculate on the possibility for nebulization delivery. Similar to what was observed in the TKA studies, there was no dose proportionality in the effect of the treatment; i.e., no significant differences were observed between the lowest (50 mg/kg bw) and the highest dose (500 mg/kg bw), suggesting that the lowest efficacious dose has not yet been defined and that once an effective dose has been reached, further increase may not be needed.

The mode of action of VOMG is novel; transcriptional analysis revealed inhibition of key metabolic pathways, such as CD, protein synthesis, ATP production, and gene transcription. Genes encoding FtsZ and other CD proteins are the most downregulated in the presence of VOMG, pointing out a possible FtsZ inhibition. Single-cell analysis and biochemical assays confirmed that VOMG affects the organisation of FtsZ polymers and, consequently, CD.

FtsZ is highly conserved among microorganisms [26], which is consistent with the broad-spectrum activity observed for VOMG. The mechanism of action of VOMG seems to be very peculiar since it is not only able to block FtsZ GTPase activity, but also to modify the polymerization kinetics of the protein which, overall, reflect an alteration of *in vivo* CD organisation and assembly rate.

VOMG has a distinct impact on the polymerization of *Mab* and *Sau* FtsZ proteins. This could be due to the low identity percentage of the C-terminal region of the two proteins, implicated in protofilament formation and in lateral interactions of polymers [67]. Interestingly, the FtsZ inhibitor PC190723, which is active against *Sau* and *Bacillus subtilis*, has been reported to induce the polymer stabilisation and suppress *in vivo* FtsZ polymer dynamics [68], similarly to the effect of VOMG on *Sau* FtsZ.

This compound also increases the rate at which *Mab* FtsZ polymerizes for a short time and then decreases it. This feature could be beneficial in a multidrug regimen: VOMG could increase the polymerisation rate, then leading to increased extracellular growth rate becoming more sensitive to VOMG and other co-administered drugs targeting actively growing bacteria.

Although several FtsZ inhibitors have been identified [29,30] in recent years, none of them are currently under development as anti-*Mab* compounds in any stage of the process.

In conclusion, VOMG is a new water-soluble compound specifically developed against *Mab* with good *in vitro, in vivo* and ADME/Tox properties and a novel mode of action specific for bacteria,

inhibiting CD. These features bring promise for a new drug candidate with the possibility to use different formulations in the much needed and narrow *Mab* drug development pipeline. Potential progression of VOMG into the clinic might bring new therapeutic options to treat lung disease caused by this pathogen and other susceptible microorganisms.

Declarations

Funding: This work was supported by: Italian Cystic Fibrosis Research Foundation grants: FFC#19/2018 (adopted by Delegazione FFC di Brindisi Torre, Delegazione FFC di Ascoli Piceno, Delegazione FFC di Novara) (MRP); FFC#14/2020 (adopted by Smartform/Tattooform, Delegazione FFC di Belluno con i rocciatori di Fonzaso) (MRP, VM, SRG, ET); FFC#18/2021 (adopted by Delegazione FFC Ricerca di Codogno e Piacenza, Delegazione FFC Ricerca di Rovigo, Delegazione FFC Ricerca di Belluno, Nonno Nanni Latteria Montello) (MRP, VM, SRG, ET); FFC#09/2023 (adopted by Carolina Sabatini, Delegazione FFC Ricerca di Siniscola Nuoro, Gruppo di sostegno FFC Ricerca di Casale Monferrato, Delegazione FFC Ricerca della Valdadige, Delegazione FFC Ricerca di Crevalcore) (MRP, FS). This work was partially supported by NextGenerationEU-MUR PNRR Extended Partnership initiative on Emerging Infectious Diseases (project no. PE00000007, INF-ACT) (MRP). L.M-M was supported by a fellowship from the Government of Aragon (Gobierno de Aragón y Fondos FEDER de la Unión Europea "Construyendo Europa desde Aragón"). J.M.E-A was funded by a fellowship from the Spanish Government (Programa de Formación de Profesorado Universitario) Ref. FPU18/03873.

Competing Interests: Patent (GD, OR, VM, MRP) related to this work has been filed (P2245IT, PCT/EP2023/078712). The other authors declare no other competing interests.

Ethical Approval: Animal work for the evaluation of pharmacokinetics and toxicity was performed under protocols approved by the Animal Care and Use Committee of the Research Centre of Biotechnology RAS (Moscow, Russia) according to the centre's guidelines for animal use, the state industry standards GOST 33044-2014, GOST 33215-2014 and GOST 33216-2014, the European Directive 2010/63/EC for animal experiments, and Guide for the Care and Use of Laboratory Animals. 8th edition (Washington (DC): National Academies Press (US); 2011). Animal studies for *in vivo* infection were conducted according to protocols and adhering strictly to the Italian Ministry of Health guidelines for the use and care of experimental animals (IACUC N°1242) and approved by the San Raffaele Scientific Institute Institutional Animal Care and Use Committee (IACUC).

Sequence Information: The RNA-seq data have been deposited in the NCBI Sequence Read Archive database under BioProject accession number SUB13481799 (BioSample accessions: SAMN35540038, SAMN35540039, SAMN35540040, SAMN35540041, SAMN35540042, SAMN35540043, SAMN35540044, SAMN35540045, SAMN35540046).

Acknowledgments

We thank Stewart Cole (Pasteur Institute, Paris, France) and Claudia Sala (Fondazione Toscana Life Sciences, Siena, Italy) for providing NTM strains and *M. abscessus* MDR clinical isolate n. 1. We also thank Dr. Ersilia V. Fiscarelli (Ospedale Pediatrico Bambino Gesù, Rome, Italy) and Dr. Lanfranco Fattorini (ISS, Rome, Italy) for giving *M. abscessus* MDR clinical isolate n. 2 and NTM drug resistant clinical isolates, respectively. We also thank Dr. Anna Egorova (Federal Research Centre "Fundamentals of Biotechnology" of the Russian Academy of Sciences, Russia) for the fruitful discussion during the drafting of the manuscript.

Supplementary materials

Supplementary material associated with this article can be found, in the online version, at …

References

[1] Boudehen Y, Kremer L. Microbe of the month: *Mycobacterium abscessus*. Trends Microbiol 2021;29:951–952. doi:10.1016/j.tim.2021.06.006.

[2] Bryant JM, Brown KP, Burbaud S, Everall I, Belardinelli JM, Rodriguez-Rincon D, et al. Stepwise pathogenic evolution of *Mycobacterium abscessus*. Science 2021;372:eabb8699. doi:10.1126/science.abb8699.

[3] Degiacomi G, Sammartino JC, Chiarelli LR, Riabova O, Makarov V, Pasca MR. *Mycobacterium abscessus*, an emerging and worrisome pathogen among cystic fibrosis patients. Int J Mol Sci 2019;20:5868. doi:10.3390/ijms24054635.

[4] Johansen MD, Herrmann JL, Kremer L. Non-tuberculous mycobacteria and the rise of *Mycobacterium abscessus*. Nat Rev Microbiol 2020;18:392-407. doi:10.1038/s41579-020-0331-1.

[5] Martiniano SL, Nick JA, Daley CL. Nontuberculous mycobacterial infections in cystic fibrosis. Clin Chest Med 2022;43:697-716. doi:10.1016/j.ccm.2015.11.001.

[6] Nguyen TQ, Heo BE, Jeon S, Ash A, Lee H, Moon C, Jang J. Exploring antibiotic resistance mechanisms in Mycobacterium abscessus for enhanced therapeutic approaches. Front Microbiol. 2024;15:1331508. doi: 10.3389/fmicb.2024.1331508.

[7] Ciofu, O, Tolker-Nielsen T, Jensen PØ, Wang H, Høiby N. Antimicrobial resistance, respiratory tract infections and role of biofilms in lung infections in cystic fibrosis patients. Adv. Drug Deliv. Rev. 2015;85:7-23. doi: 10.1016/j.addr.2014.11.017

[8] Uruén C, Chopo-Escuin G, Tommassen J, Mainar-Jaime RC, Arenas, J. Biofilms as promoters of bacterial antibiotic resistance and tolerance. Antibiotics, 2020;10:3. doi: 10.3390/antibiotics10010003.

[9] Nasrollahian S, Pourmoshtagh H, Sabour S, Hadi N, Azimi T, Soleiman-Meigooni S. Biofilm formation in mycobacterial genus; mechanism of biofilm formation and anti-mycobacterial biofilm agents. Curr Pharm Biotechnol. 2024. doi: 10.2174/0113892010277107240227054933

[10] Daley CL, Iaccarino JM, Lange C, Cambau E, Wallace RJ Jr, Andrejak C, et al. Treatment of nontuberculous mycobacterial pulmonary disease: an official ATS/ERS/ESCMID/IDSA clinical practice guideline. Clin Infect Dis 2020;71:e1-e36. doi:10.1183/13993003.00535-2020.

[11] Fröberg G, Maurer FP, Chryssanthou E, Fernström L, Benmansour H, Boarbi S, et al. EUCAST AMST & ESCMYC study groups. Towards clinical breakpoints for non-tuberculous mycobacteria - Determination of epidemiological cut off values for the *Mycobacterium avium* complex and *Mycobacterium abscessus* using broth microdilution. Clin Microbiol Infect 2023;29:758-764. doi:10.1016/j.cmi.2023.02.007.

[12] Luthra S, Rominski A, Sander P. The role of antibiotic-target-modifying and antibiotic-modifying enzymes in *Mycobacterium abscessus* drug resistance. Front Microbiol 2018;9:2179. doi:10.3389/fmicb.2018.02179.

[13] Egorova A, Jackson M, Gavrilyuk V, Makarov V. Pipeline of anti-*Mycobacterium abscessus* small molecules: repurposable drugs and promising novel chemical entities. Med Res Rev 2021;41:2350-2387. doi:10.1002/med.21798.

[14] Tunesi S, Zelazny A, Awad Z, Mougari F, Buyck JM, Cambau E. Antimicrobial susceptibility of *Mycobacterium abscessus* and treatment of pulmonary and extra-pulmonary infections. Clin Microbiol Infect 2023;S1198-743X(23)00482-2. doi:10.1016/j.cmi.2023.09.019.

[15] Wiesel V, Aviram M, Mei-Zahav M, Dotan M, Prais D, Cohen-Cymberknoh M, Gur M, Bar-Yoseph R, Livnat G, Goldbart A, Hazan G, Hazan I, Golan-Tripto I. Eradication of nontuberculous mycobacteria in people with cystic fibrosis treated with elexacaftor/tezacaftor/ivacaftor: a multicenter cohort study. J Cyst Fibros. 2024;23:41-49. doi: 10.1016/j.jcf.2023.05.003.

[16] Gavey R, Nolan J, Moore V, Reid D, Brown J. Clinical and radiological improvement of cavitary *Mycobacteroides abscessus* disease in cystic fibrosis following initiation of elexacaftor/tezacaftor/ivacaftor. J Cyst Fibros. 2024;21:S1569-1993(24)00071-7. doi: 10.1016/j.jcf.2024.05.008.

[17] Belardinelli JM, Verma D, Li W, Avanzi C, Wiersma CJ, Williams JT, et al. Therapeutic efficacy of antimalarial drugs targeting DosRS signaling in *Mycobacterium abscessus*. Sci Transl Med 2022;14:eabj3860. doi:10.1126/scitranslmed.abj3860.

[18] Li A, He S, Li J, Zhang Z, Li B, Chu H. Omadacycline, eravacycline, and tigecycline express anti-*Mycobacterium abscessus* activity *in vitro*. Microbiol Spectr 2023;4:e0071823. doi10.1128/spectrum.00718-23.

[19] Nguyen TQ, Heo BE, Hanh BTB, Jeon S, Park Y, Choudhary A, et al. DS86760016, a leucyl-tRNA synthetase inhibitor, is active against *Mycobacterium abscessus*. Antimicrob Agents Chemother 2023;22:e0156722. doi:10.1128/aac.01567-22.

[20] Rimal B, Batchelder HR, Story-Roller E, Panthi CM, Tabor C, Nuermberger EL, et al. T405, a new penem, exhibits in vivo efficacy against *M. abscessus* and synergy with β-lactams imipenem and cefditoren. Antimicrob Agents Chemother 2022;66:e0053622. doi:10.1128%2Faac.00536-22

[21] Negatu DA, Beuchel A, Madani A, Alvarez N, Chen C, Aragaw WW, et alPiperidine-4-carboxamides target DNA gyrase in *Mycobacterium abscessus*. Antimicrob Agents Chemother 2021;65:e0067621. doi.org/10.1128/aac.00676-21.

[22] Lang M, Ganapathy US, Mann L, Abdelaziz R, Seidel RW, Goddard R, et al. Synthesis and characterization of phenylalanine amides active against *Mycobacterium abscessus* and other mycobacteria. J Med Chem 2023;66:5079-5098. doi:10.1021/acs.jmedchem.3c00009.

[23] Zhang K, Limwongyut J, Moreland AS, Wei SCJ, Jim Jia Min T, Sun Y, et al. An anti-mycobacterial conjugated oligoelectrolyte effective against *Mycobacterium abscessus*. Sci Transl Med. 2024;16:eadi7558. doi: 10.1126/scitranslmed.adi7558.

[24] den Blaauwen T, Andreu JM, Monasterio O. Bacterial cell division proteins as antibiotic targets. Bioorg Chem. 2014;55:27-38. doi:10.1016/j.bioorg.2014.03.007.

[25] Donovan C, Bramkamp M. Cell division in *Corynebacterineae*. Front Microbiol 2014;5:132. doi:10.3389%2Ffmicb.2014.00132.

[26] Pradhan P, Margolin W, Beuria TK. Targeting the Achilles heel of FtsZ: the interdomain cleft. Front Microbiol 2021;12:732796. doi:10.3389/fmicb.2021.732796.

[27] Han H, Wang Z, Li T, Teng D, Mao R, Hao Y, et al. Recent progress of bacterial FtsZ inhibitors with a focus on peptides. FEBS J 2021;288:1091-1106. doi:10.1111/febs.15489.

[28] Shinde Y, Pathan A, Chinnam S, Rathod G, Patil B, Dhangar M, Mathew B, Kim H, Mundada A, Kukreti N, Ahmad I, Patel H. Mycobacterial FtsZ and inhibitors: a promising target for the anti-tubercular drug development. Mol. Divers. 2023. doi: 10.1007/s11030-023-10759-8

[29] Hogan AM, Scoffone VC, Makarov V, Gislason AS, Tesfu H, Stietz MS, et al. Competitive fitness of essential gene knockdowns reveals a broad-spectrum antibacterial inhibitor of the cell division protein FtsZ. Antimicrob Agents Chemother 2018;62:e01231-18. doi:10.1128/aac.01231-18.

[30] Low JL, Wu ML, Aziz DB, Laleu B, Dick T. Screening of TB Actives for activity against nontuberculous mycobacteria delivers high hit rates. Front Microbiol 2017;8:1539. doi:10.3389/fmicb.2017.01539.

[31] Schneider CA, Rasband WS, Eliceiri KW. NIH Image to ImageJ: 25 years of image analysis. Nat Methods 2012;9:671-675. doi:10.1038/nmeth.2089.

[32] Król E, Scheffers DJ. FtsZ polymerization assays: simple protocols and considerations. J Vis Exp 2013;81:e50844. doi:10.3791%2F50844.

[33] Trespidi G, Scoffone VC, Barbieri G, Marchesini F, Abualsha'ar A, Coenye T, et al. Antistaphylococcal activity of the FtsZ inhibitor C109. Pathogens 2021;10:886. doi:10.3390/pathogens10070886.

[34] Saliu F, Rizzo G, Bragonzi A, Cariani L, Cirillo DM, Colombo C, et al. Chronic infection by nontypeable *Haemophilus influenzae* fuels airway inflammation. ERJ Open Res. 2021;7:00614-2020. doi:10.1183/23120541.00614-2020.

[35] Lorè NI, Saliu F, Spitaleri A, Schäfle D, Nicola F, Cirillo DM, Sander P. The aminoglycoside-modifying enzyme Eis2 represents a new potential *in vivo* target for reducing antimicrobial drug resistance in *Mycobacterium abscessus* complex. Eur Respir J 2022;60:2201541. doi:10.1183/13993003.01541-2022.

[36] Nicola F, Cirillo DM, Lorè NI. Preclinical murine models to study lung infection with *Mycobacterium abscessus* complex. Tuberculosis 2023;138:102301. doi:10.1016/j.tube.2022.102301.

[37] Riva C, Tortoli E, Cugnata F, Sanvito F, Esposito A, Rossi M, et al. A New Model of Chronic *Mycobacterium abscessus* Lung Infection in Immunocompetent Mice. Int J Mol Sci 2020;21:6590. doi:10.3390/ijms21186590.

[38] Salina EG, Ryabova O, Vocat A, Nikonenko B, Cole ST, Makarov V. New 1-hydroxy-2-thiopyridine derivatives active against both replicating and dormant *Mycobacterium tuberculosis*. J Infect Chemother 2017;23:794-797. doi:10.1016/j.jiac.2017.04.012.

[39] Muñoz-Egea MC, García-Pedrazuela M, Mahillo I, Esteban J. Effect of ciprofloxacin in the ultrastructure and development of biofilms formed by rapidly growing mycobacteria. BMC Microbiol. 2015;15:18. doi: https://doi.org/10.1186%2Fs12866-015-0359-y.

[40] Castañeda-García A, Prieto AI, Rodríguez-Beltrán J, Alonso N, Cantillon D, Costas C, et al. A non-canonical mismatch repair pathway in prokaryotes. Nat Commun 2017;8:14246. doi:10.1038/ncomms14246.

[41] Makarov V, Manina G, Mikusova K, Möllmann U, Ryabova O, Saint-Joanis B, et al. Benzothiazinones kill *Mycobacterium tuberculosis* by blocking arabinan synthesis. Science 2009;324:801-804. doi:10.1126/science.1171583.

[42] Poce G, Bates RH, Alfonso S, Cocozza M, Porretta GC, Ballell L, et al. Improved BM212 MmpL3 inhibitor analogue shows efficacy in acute murine model of tuberculosis infection. PLoS One 2013;8:e56980. doi:10.1371/journal.pone.0056980.

[43] Mori G, Chiarelli LR, Esposito M, Makarov V, Bellinzoni M, Hartkoorn RC, et al. Thiophenecarboxamide derivatives activated by EthA kill *Mycobacterium tuberculosis* by inhibiting the CTP synthetase PyrG. Chem Biol 2015;22:917-927. doi:10.1016/j.chembiol.2015.05.016.

[44] Chiarelli LR, Mori G, Orena BS, Esposito M, Lane T, de Jesus Lopes Ribeiro AL, et al. A multitarget approach to drug discovery inhibiting *Mycobacterium tuberculosis* PyrG and PanK. Sci. Rep. 2018;8:3187. doi:10.1038/s41598-018-21614-4.

[45] Albesa-Jové D, Chiarelli LR, Makarov V, Pasca MR, Urresti S, Mori G, et al. Rv2466c mediates the activation of TP053 to kill replicating and non-replicating *Mycobacterium tuberculosis*. ACS Chem. Biol. 2014;9:1567-1575. doi:10.1021/cb500149m.

[46] Mori G, Orena BS, Chiarelli LR, Degiacomi G, Riabova O, Sammartino JC, et al. Rv0579 is involved in the resistance to the TP053 antitubercular prodrug. Front Microbiol 2020;11:292. doi:10.3389/fmicb.2020.00292.

[47] Neres J, Hartkoorn RC, Chiarelli LR, Gadupudi R, Pasca MR, Mori G, et al. 2-Carboxyquinoxalines kill *Mycobacterium tuberculosis* through noncovalent inhibition of DprE1. ACS Chem Biol 2015;10:705-714. doi:10.1021/cb5007163.

[48] Kapopoulou A, Lew JM, Cole ST. The MycoBrowser portal: a comprehensive and manually annotated resource for mycobacterial genomes. Tuberculosis 2011;91:8-13. doi: 10.1016/j.tube.2010.09.006.

[49] Schildkraut JA, Coolen JPM, Burbaud S, Sangen JJN, Kwint MP, Floto RA, et al. RNA sequencing elucidates drug-specific mechanisms of antibiotic tolerance and resistance in *Mycobacterium abscessus*. Antimicrob Agents Chemother 2022;66:e0150921. doi:10.1128/aac.01509-21.

[50] Koul A, Vranckx L, Dhar N, Göhlmann HW, Özdemir E, Neefs JM, et al. Delayed bactericidal response of *Mycobacterium tuberculosis* to bedaquiline involves remodelling of bacterial metabolism. Nat Commun 2014;5:3369. doi:10.1038/ncomms4369

[51] McNeil MB, Ryburn HWK, Harold LK, Tirados JF, Cook GM. Transcriptional inhibition of the F1F0-Type ATP synthase has bactericidal consequences on the viability of mycobacteria. Antimicrob Agents Chemother 2020;64:e00492-20. doi:10.1128/aac.00492-20.

[52] Klepp LI, Sabio y Garcia J, Bigi F. Mycobacterial MCE proteins as transporters that control lipid homeostasis of the cell wall. Tuberculosis 2022;132:102162. doi:10.1016/j.tube.2021.102162.

[53] Santi I, Dhar N, Bousbaine D, Wakamoto Y, McKinney JD. Single-cell dynamics of the chromosome replication and cell division cycles in mycobacteria. Nat Commun 2013;4:2470. doi:10.1038/ncomms3470.

[54] Dedrick RM, Smith BE, Cristinziano M, Freeman KG, Jacobs-Sera D, Belessis Y, et al. Phage therapy of mycobacterium infections: compassionate use of phages in 20 patients with drug-resistant mycobacterial disease. Clin Infect Dis 2023;76:103-112. doi:10.1093/cid/ciac453.

[55] Bhat, Z. S., Rather, M. A., Maqbool, M., Lah, H. U., Yousuf, S. K., & Ahmad, Z. (2017). Cell wall: A versatile fountain of drug targets in Mycobacterium tuberculosis. Biomedicine & Pharmacotherapy, 95, 1520-1534.

[56] Machado, D., Girardini, M., Viveiros, M., & Pieroni, M. (2018). Challenging the drug-likeness dogma for new drug discovery in tuberculosis. Frontiers in microbiology, 9, 383242.

[57] Dupont CL, Grass G, Rensing C. Copper toxicity and the origin of bacterial resistance-new insights and applications. Metallomics 2011;3:1109-1118. doi:10.1039/c1mt00107h.

[58] Dalecki AG, Crawford CL, Wolschendorf F. Copper and Antibiotics: Discovery, Modes of Action, and Opportunities for Medicinal Applications. Adv Microb Physiol 2017;70:193-260. doi:10.1016/bs.ampbs.2017.01.007.

[59] Banaschewski B, Verma D, Pennings LJ, Zimmerman M, Ye Q, Gadawa J, et alClofazimine inhalation suspension for the aerosol treatment of pulmonary nontuberculous mycobacterial infections. J Cyst Fibros . 2019;18:714-720. doi:10.1016/j.jcf.2019.05.013.

[60] Pasca MR, Degiacomi G, Riabova O, Makarov V. Pyridine-2-thiol 1-oxide derivatives and their use for treatment of mammalian infections caused by mycobacterium or fungi. 2022 Italian patent application number P2245IT. PCT/EP2023/078712.

[61] Kwak N, Dalcolmo MP, Daley CL, Eather G, Gayoso R, Hasegawa N, et al. *Mycobacterium abscessus* pulmonary disease: individual patient data meta-analysis. Eur Respir J 2019;54:1801991. doi:10.1183/13993003.01991-2018.

[62] Wu ML, Aziz DB, Dartois V, Dick T. NTM drug discovery: status, gaps and the way forward. Drug Discov Today 2018;23:1502-1519. doi:10.1016/j.drudis.2018.04.001.

[63] Wu W, He S, Li A, Guo Q, Tan Z, Liu S, et al. A novel leucyl-tRNA synthetase inhibitor, MRX-6038, expresses anti-*Mycobacterium abscessus* activity *in vitro* and *in vivo*. Antimicrob Agents Chemother 2022;66:e0060122. doi:10.1128%2Faac.00601-22.

[64] Flores VD, Siqueira FD, Mizdal CR, Bonez PC, Agertt VA, Stefanello ST., et al. Antibiofilm effect of antimicrobials used in the therapy of mycobacteriosis. Microb Pathog 2016;99:229-235. doi:10.1016/j.micpath.2016.08.017.

[65] Maggioncalda EC, Story-Roller E, Mylius J, Illei P, Basaraba RJ, Lamichhane G. A mouse model of pulmonary *Mycobacteroides abscessus* infection. Sci Rep 2020;10:3690. doi:10.1038/s41598-020-60452-1-

[66] Rimal B, Batchelder HR, Story-Roller E, Panthi CM, Tabor C, Nuermberger EL, et al. T405, a new penem, exhibits *in vivo* efficacy against *M. abscessus* and synergy with β-lactams imipenem and cefditoren. Antimicrob Agents Chemother 2022;66:e0053622. doi:10.1128/aac.00536-22.

[67] Silber N, Matos de Opitz CL, Mayer C, Sass P. Cell division protein FtsZ: from structure and mechanism to antibiotic target. Future Microbiol 2020;15:801-831. doi:10.2217/fmb-2019-0348.

[68] Andreu JM, Schaffner-Barbero C, Huecas S, Alonso D, Lopez-Rodriguez ML, Ruiz-Avila LB, et al. The antibacterial cell division inhibitor PC190723 is an FtsZ polymer-stabilizing agent that induces filament assembly and condensation. J Biol Chem 2010;285:14239-14246. doi:10.1074/jbc.m109.094722.

Figures

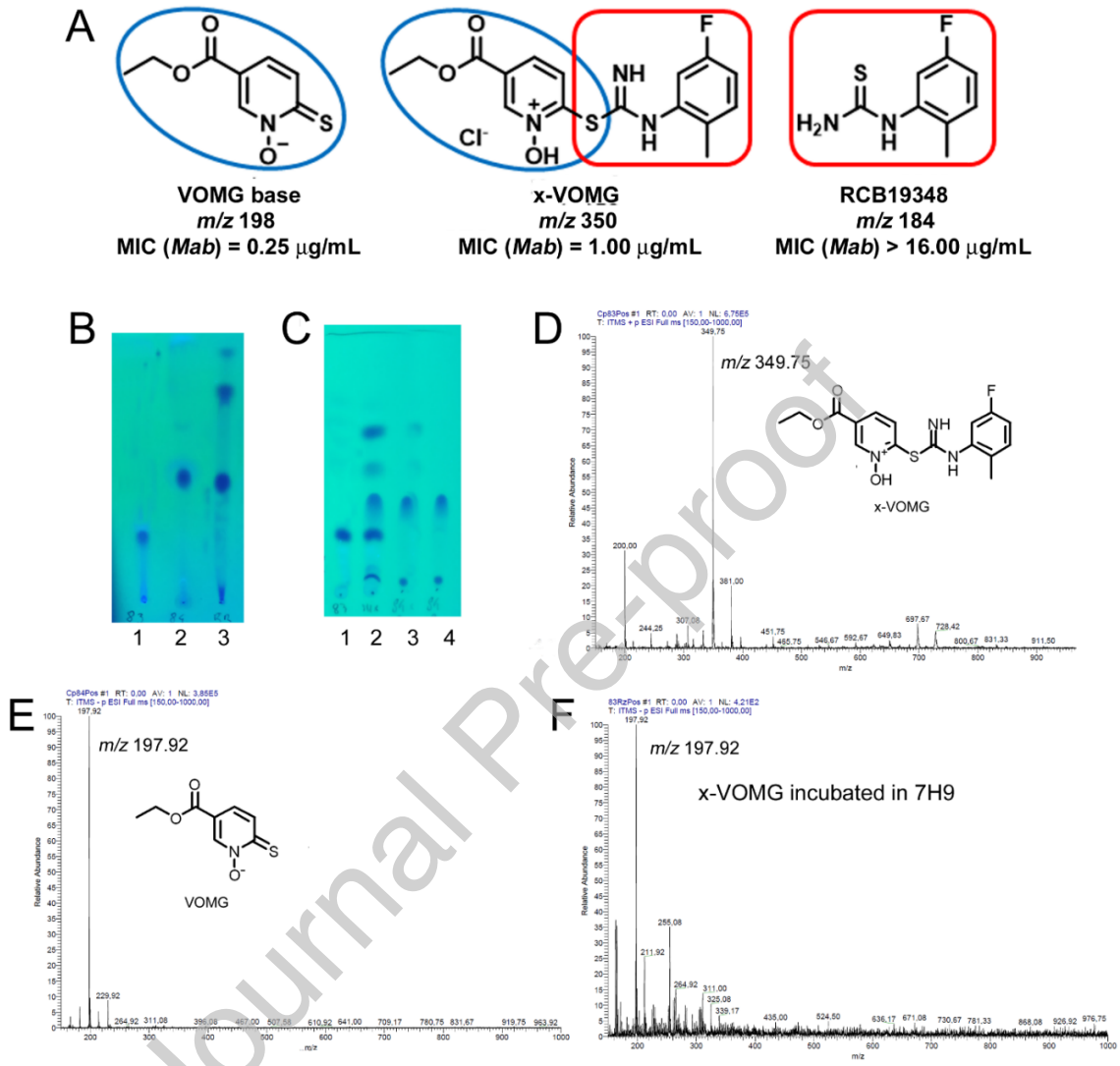

Fig. 1. Discovery of VOMG as the active metabolite of x-VOMG.

A, Transformation of x-VOMG in its metabolites, including VOMG. **B**, TLC analysis of the extracts of *M. smegmatis* cultures treated with the compounds. 1: x-VOMG; 2: VOMG; 3: extract of culture treated with x-VOMG. **C**, TLC analysis of the compounds, after 24 hours incubation in 7H9 medium. 1: x-VOMG; 2: x-VOMG extracted after incubation in 7H9; 3: VOMG extracted after incubation in 7H9; 4: VOMG. **D**, Mass spectrometry analysis of x-VOMG. **E**, Mass spectrometry analysis of VOMG. **F**, Mass spectrometry analysis of x-VOMG extracted after incubation in 7H9 medium.

A

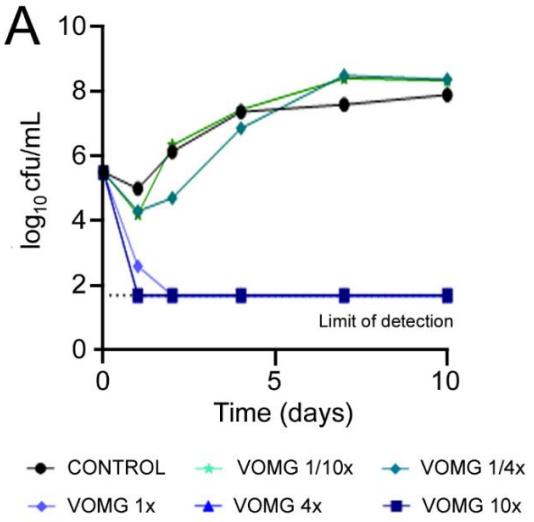

B

Compounds	Activity against *Mab* ATCC 19977 (μg/mL)	
	MIC	MBEC
x-VOMG	1.00	256.00
VOMG	0.25	128.25
Clarithromycin	4.00	128.00
Amikacin	32.00	64.00

C

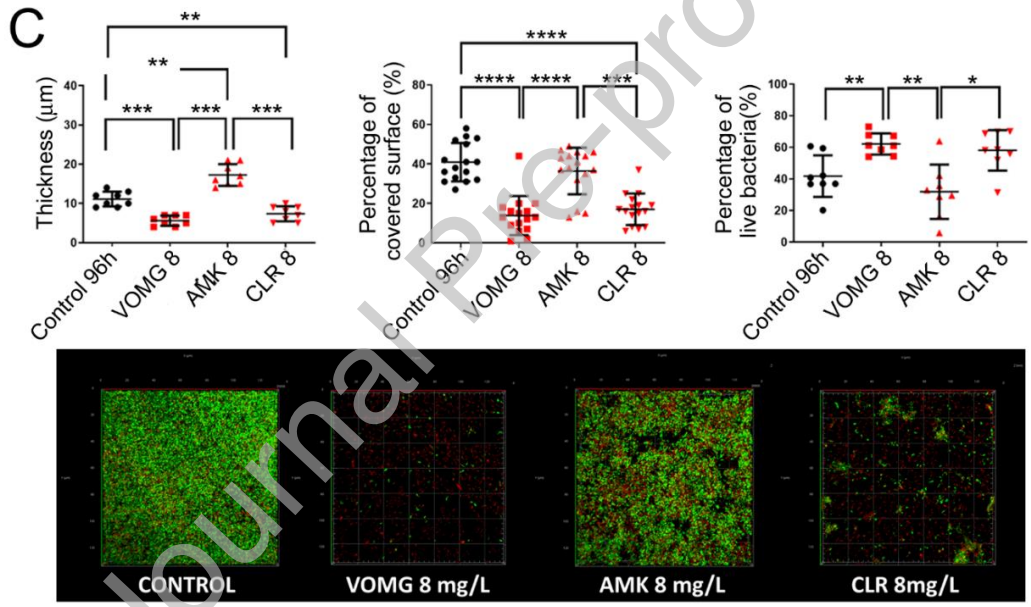

Fig. 2. VOMG has bactericidal and anti-biofilm activity against *Mab*.
A, Time killing assay of VOMG in *Mab*. The graph is representative of three different experiments (each experiment includes two technical replicates). **B**, Minimum inhibitory concentration (MIC) and minimum biofilm eradication concentration (MBEC) of VOMG and x-VOMG against *Mab*. **C**, Prevention of biofilm formation with VOMG, clarithromycin and amikacin at 8 μg/mL.

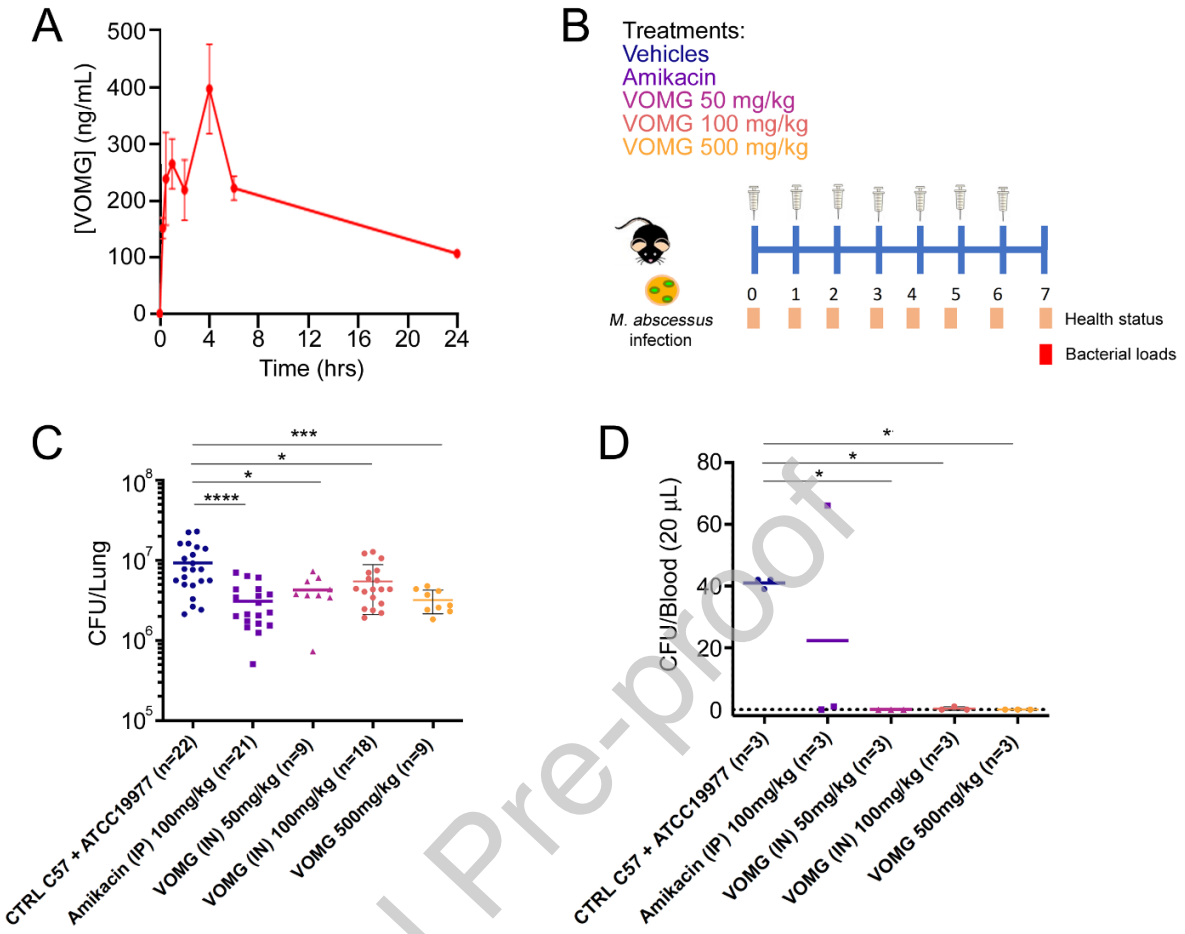

Fig. 3. VOMG had a good bioavailability and it is effective *in vivo*.
A, Pharmacokinetics of VOMG after 100 mg/kg *per os* administration in mice. **B**, Evaluation of the efficacy of VOMG (50, 100 and 500 mg/kg) in immunocompetent C57BL/6NCrl mice infected with agar-embedded *Mab* cells by intranasal administration. Amikacin (100 mg/kg, IP) was used as internal control. Timeline of the experiment. **C**, VOMG at 50, 100 and 500 mg/kg, significantly reduced the bacterial burden in the lungs compared with infected groups. **D**, A similar trend in bacterial burden reduction after VOMG treatment was observed in blood samples.

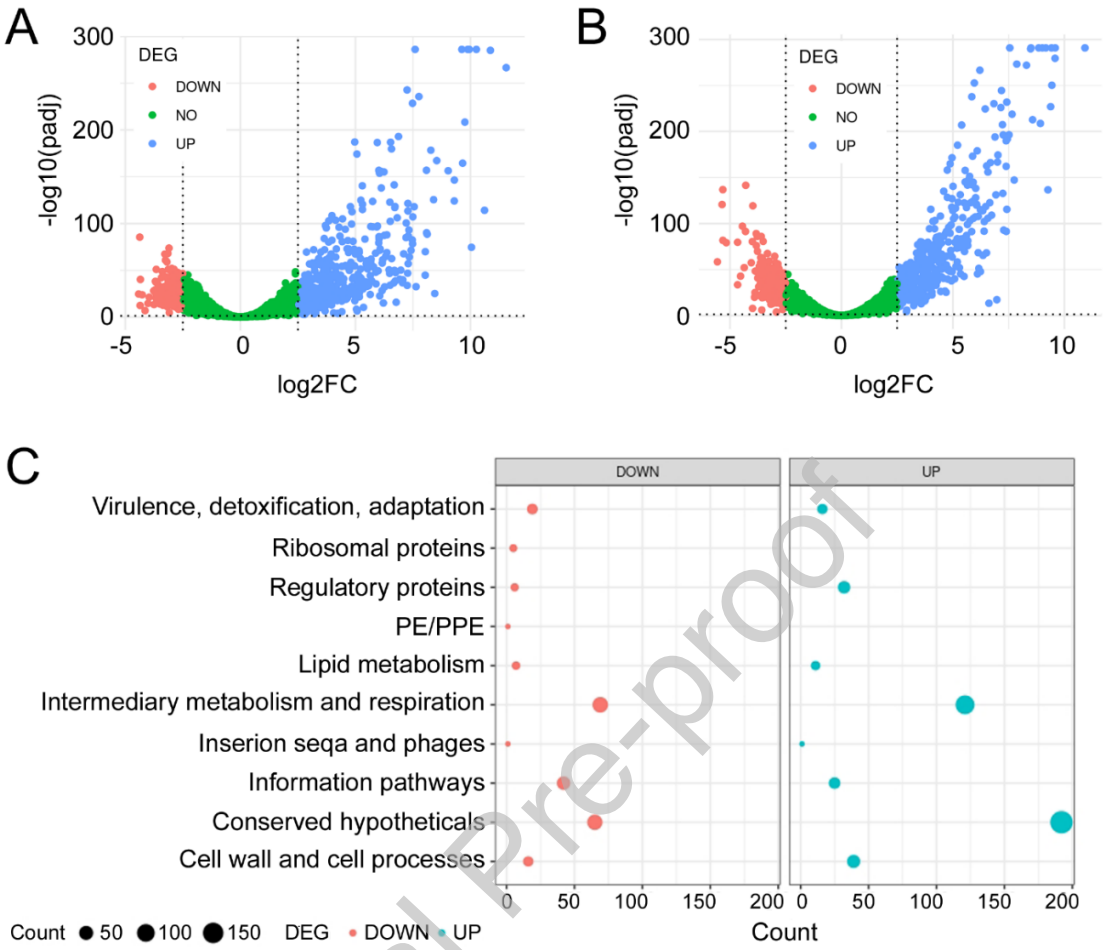

Fig. 4. x-VOMG inhibits several key metabolic pathways, in particular cell division. **A**, Volcano plot showing *Mab* genes up- (blue) and downregulated (red) in response to x-VOMG treatment (10 μg/mL). **B**, Volcano plot showing *Mab* genes up- (blue) and downregulated (red) in response to x-VOMG treatment (20 μg/mL). **C**, COG Enrichment plot showing shared categories significantly down- (red) and upregulated (blue) in response to x-VOMG treatment. **D**, Single-cell area and length of *Mab* wild type strain either treated with 50 μg/mL of VOMG or not for 4 hours. On the right, representative snapshot images of *Mab* wild type strain either treated with 50 μg/mL of VOMG or not (control) for 4 hours and stained with Hoechst and FM^{TM} 1-43. **E**, Single-cell area and length of *Mab* wild type strain either treated with 50 μg/mL of VOMG or not for 24 hours. Black lines indicate mean ± SD ($83 > n < 103$). On the right, representative snapshot images of *Mab* wild type strain either treated with 50 μg/mL of VOMG or not (control) for 24 hours and stained with Hoechst and FM^{TM} 1-43. For Figures D and E, Black lines indicate mean ± SD ($83 > n < 103$). Asterisks denote significant difference by Welch t-test: **P = 0.0021; ***P = 0.0004; ****P < 0.0001. Hoechst (blue) and FM^{TM} 1-43 (yellow) are shown separately and merged, as indicated in the snapshots. Scale bar 2 μm.

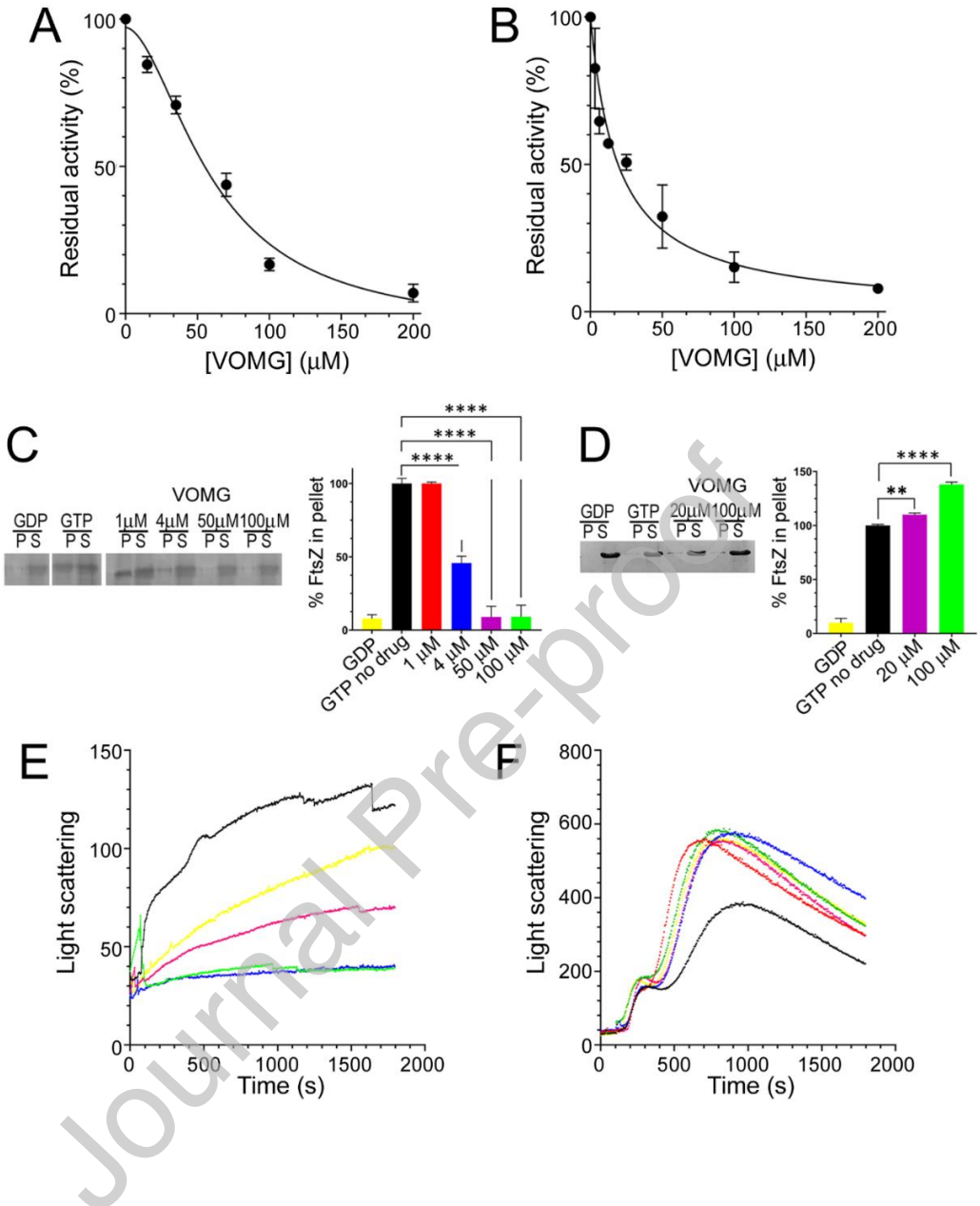

Fig. 5. VOMG inhibits FtsZ activity in both *M. abscessus* and *S. aureus*.

A, IC_{50} determination of VOMG against *Mab* FtsZ GTPase activity. Data are the mean ± SD from three different replicates. **B**, IC_{50} determination of VOMG against *S. aureus* FtsZ GTPase activity. Data are the mean ± SD from three different replicates. **C**, SDS-PAGE of the sedimentation assay of *Mab* FtsZ in the presence/absence of VOMG. **D**, SDS-PAGE of the sedimentation assay of *Sau* FtsZ in the presence/absence of VOMG. For Figures C and D, P, insoluble fraction (pellet); S, soluble fraction (supernatant). Images are representative of at least three different experiments. On the right, the densitometric analysis of the gels is reported; the density of the protein band in the pellet of the reactions performed with GTP in the absence of VOMG was used as reference and

considered as 100% (** P < 0.01, **** P < 0.0001 one-way ANOVA test). **E**, Light scattering polymerization assay of *Mab* FtsZ in absence (black line) or in presence of increasing concentration of VOMG (400 µM, red line; 200 µM, blue line; 100 µM green line; 50 µM, purple line, 25 µM, yellow line). **F**, Light scattering polymerization assay of *S. aureus FtsZ* in absence (black line) or in presence of increasing concentration of VOMG (as in Fig. E).

Graphical Abstract